Supplemental Data

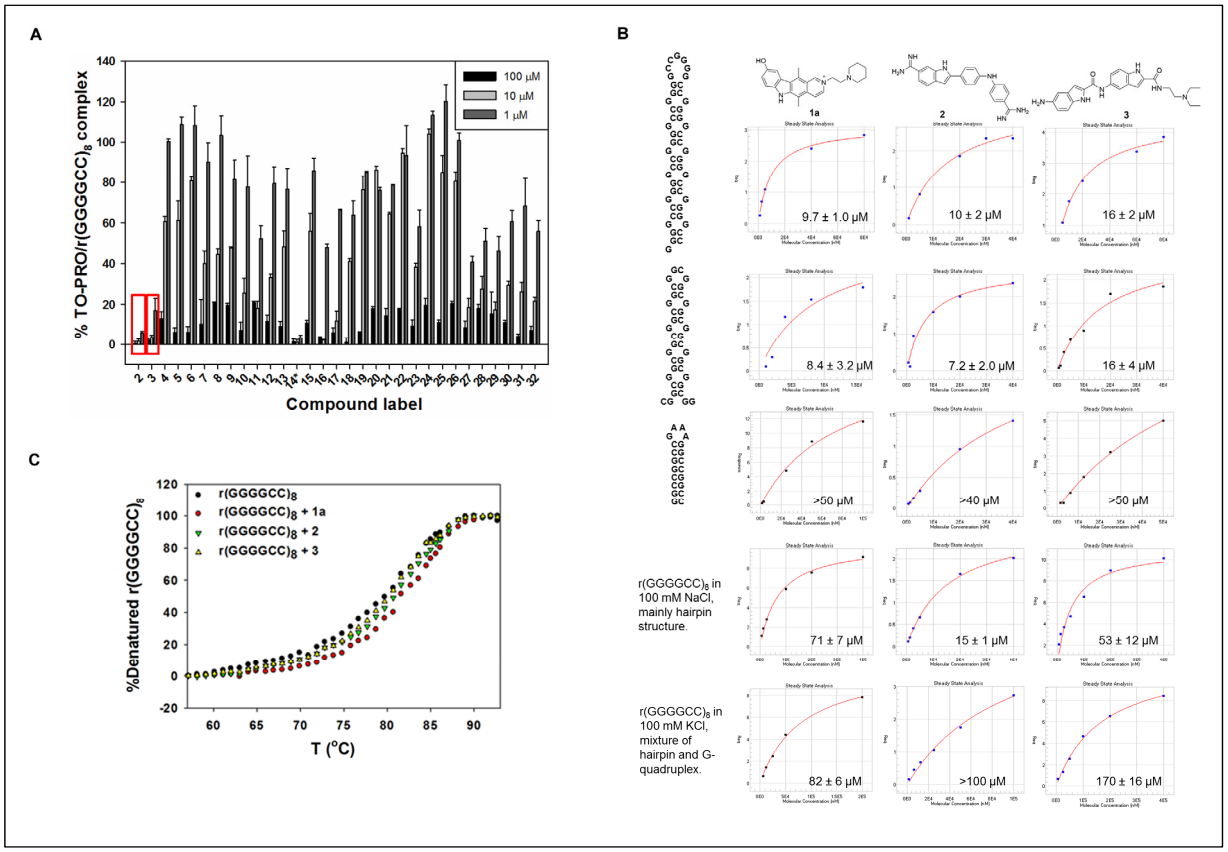

Figure S1, related to Figure 1. A) Screening for lead compounds that bind r(GGGGCC)$_8$ using a dye (TO-PRO-1) displacement assay. An initial screen completed with 100 µM compound identified 31 potential leads (from 132 total compounds) that were further refined by screening at 10 and 1 µM concentrations. Lead compounds are highlighted in red rectangles. Data are presented as mean ± SD (n=3). * Compound is unstable as determined by LC-MS. **B)** Binding affinity of lead compounds **1a**, **2**, and **3** to r(CGG)$_{12}$, r(GGCC)$_4$, and hairpin and G-quadruplex conformations of r(GGGGCC)$_8$, as determined by BLI. **C)** Optical melting experiment of r(GGGGCC)$_8$ with **1a**, **2**, and **3**. Treatment of r(GGGGCC)$_8$ with compound **1a** and **2** (1:3) stabilizes the RNA repeat and increases its melting temperature.

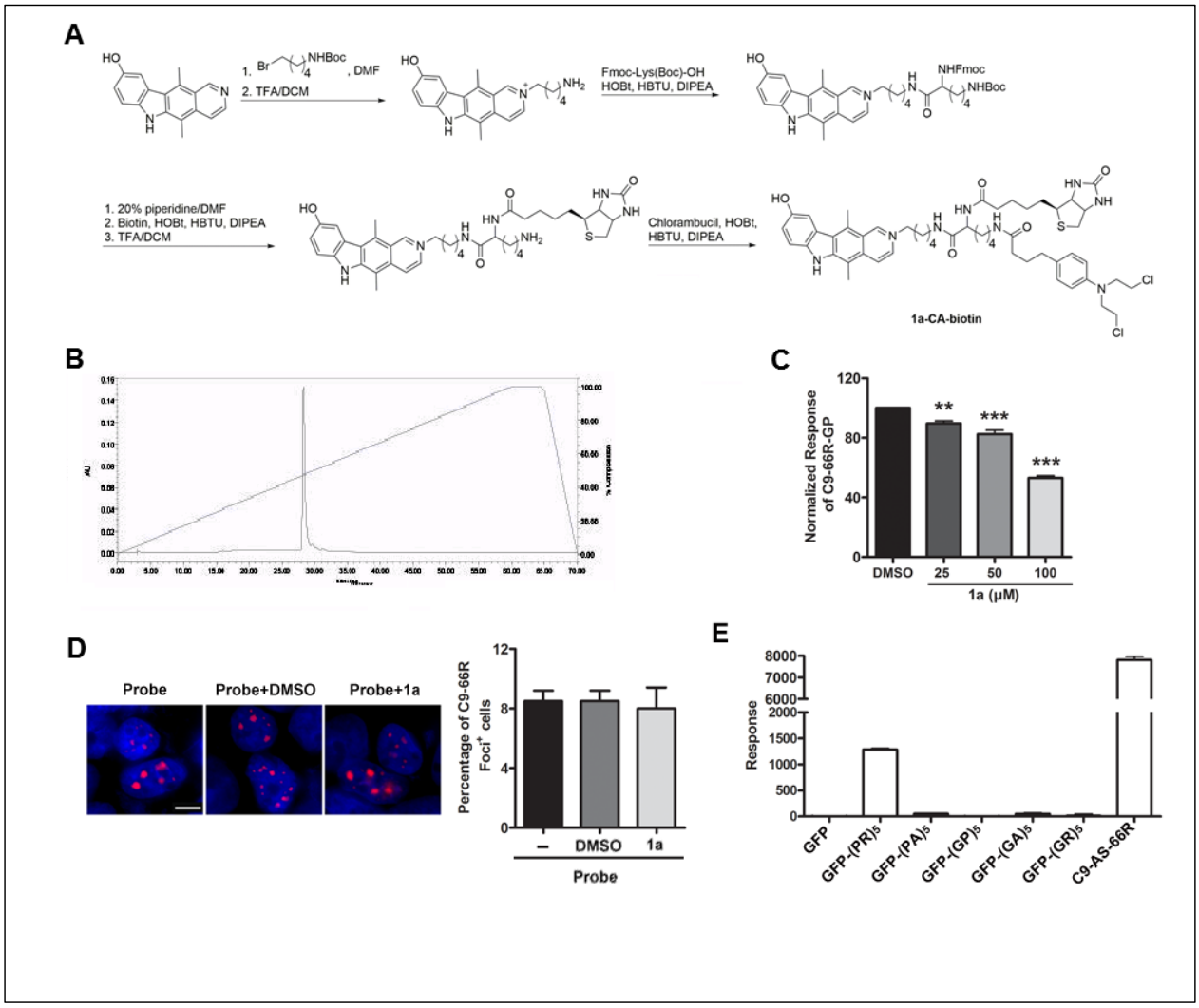

Figure S2, related to Figure 2. A-B) Synthetic route (**A**) and analytic HPLC chromatogram (**B**) for **1a-CA-Biotin. C)** $(GGGGCC)_{66}$-expressing cells were treated with DMSO or compounds **1a** (25, 50 and 100 μM) for 24 h. Poly(GP) protein expression in cell lysates was analyzed by GP immunoassay (see Fig. S4A for validation of GP assay specificity). Responses correspond to the intensity of emitted light upon electrochemical stimulation of the assay plate using the MSD Sector Imager 2400, normalized to the response in DMSO-treated cells. Data presented as mean+SEM (n=3). **P<0.01, ***P<0.001 as assessed by one-way ANOVA followed by Dunnett's Multiple Comparison Test. **D**) To determine whether the decrease in the percentage of foci-positive r$(GGGGCC)_{66}$-expressing cells following **1a** treatment is caused by inhibition of foci formation or is instead an artefact resulting from impaired binding of the FISH probe to **1a**-

bound r(GGGGCC)$_{66}$, non-treated (GGGGCC)$_{66}$-expressing cells were fixed prior to conducting RNA-FISH with a probe co-incubated with either DMSO or **1a**. Note that **1a** did not interfere with binding of the probe to r(GGGGCC)$_{66}$-containing foci. **E**) A sandwich MSD immunoassay using rabbit polyclonal anti-PR was developed. To validate specificity, lysates from cells expressing the indicated GFP-tagged dipeptide repeat proteins were assayed. Response values correspond to intensity of emitted light upon electrochemical stimulation of the assay plate using the MSD Sector Imager 2400, from which the background response in wells containing lysates from GFP-expressing cells was subtracted.

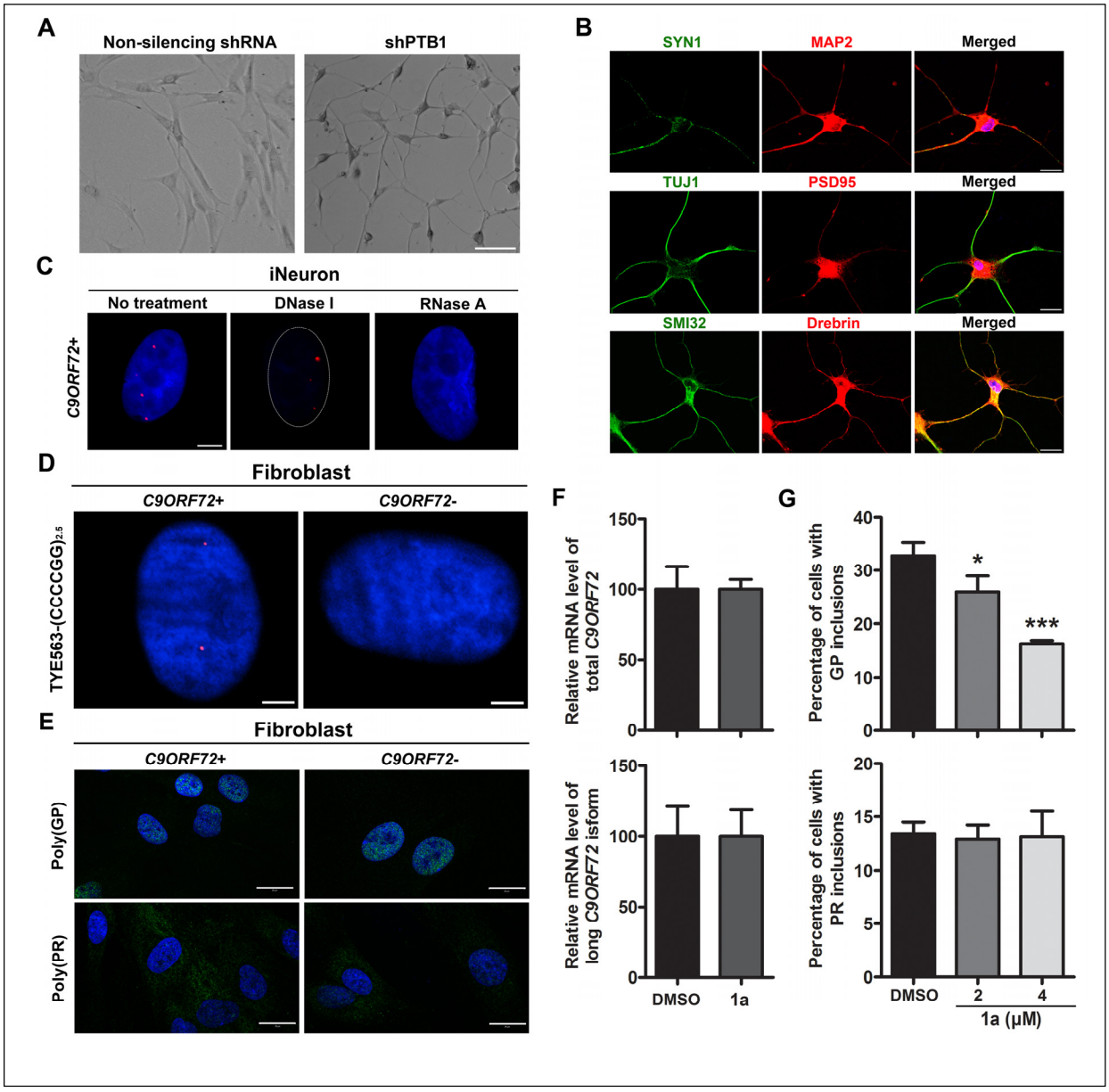

Figure S3, related to Figure 3. Human fibroblasts are converted to iNeurons following PTB1 knockdown. A) Representative bright field images show cell morphology upon control, non-silencing shRNA and shPTB1 transduction of human fibroblasts. While the cells infected with control shRNA retained their fibroblast-like shape, shPTB1-transduction induced a neuronal morphology with reduced size of cell soma, and neurite outgrowth. Scale bar, 400 μm. **B)** iNeurons express cytoskeletal neuronal markers MAP2, TUJ1 and neurofilament Smi32, as well

as synaptic markers synapsin 1 (SYN1) and post-synaptic density protein 95 (PSD95). These cells also express Drebrin, which plays a role in the formation and maintenance of dendritic spines in neurons. Scale bars, 20 μm. **C)** Nuclear foci detected in *C9ORF72*+ iNeurons are primarily composed of RNA. *C9ORF72*+ iNeurons were treated with DNase I or RNase A prior to RNA FISH using a 5′TYE563-$(CCCCGG)_{2.5}$-‘3 LNA probe. Treatment with RNAse A degraded all foci, but DNAse I only degraded nuclear DNA (observed by loss of Hoechst staining) leaving foci in iNeurons intact. Scale bars, 5 μm. **D)** As observed in *C9ORF72*+ iNeurons (**Fig.3C**) foci of (GGGGCC) repeat-containing RNA were detected in fibroblasts from individuals with the *C9ORF72* repeat expansion. Scale bars, 5 μm. **E)** In contrast to *C9ORF72*+ iNeurons (**Fig.3C**), poly(GP) and poly(PR) protein inclusions are not observed in *C9ORF72*+ fibroblasts. Scale bars, 20 μm. **F)** qRT-PCR using primers designed to target all *C9ORF72* variants, or specifically the long form of *C9ORF72*, show that treatment of iNeurons with **1a** (4 μM) does not cause a decrease in these mRNA transcripts. Data presented as mean+SEM of three *C9ORF72*+ iNeurons lines analyzed by paired t-test. **G)** A dose-dependent decrease in poly(GP) inclusions, but not poly(PR) inclusions, was observed upon treatment of *C9ORF72*+ iNeurons with **1a**. Data presented as mean+SEM (n=3). *P<0.05, ***P<0.001, as assessed by one-way ANOVA followed by Dunnett’s Multiple Comparison Test. Nuclei (blue) in all panels were stained with Hoechst 33258.

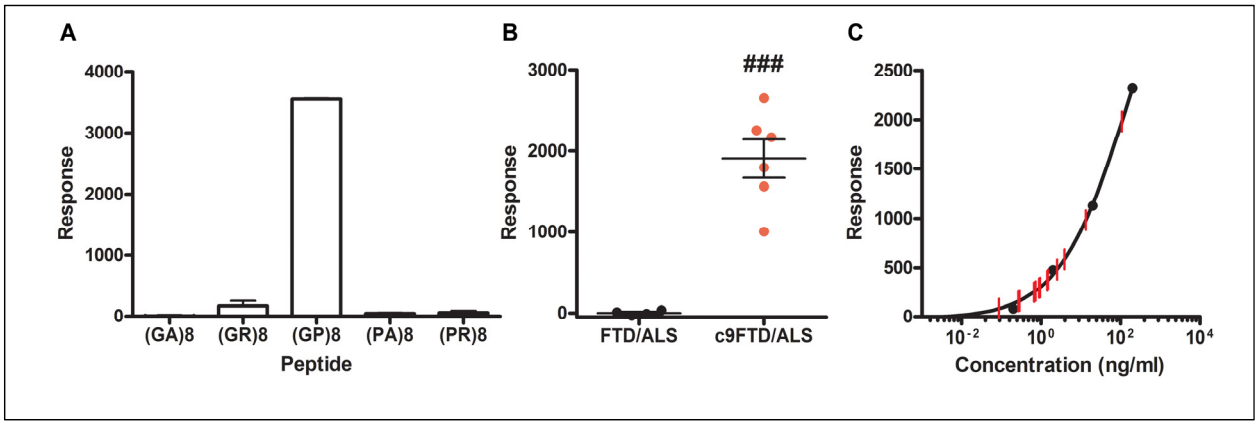

Figure S4, related to Figure 4. Validation of Poly(GP) MSD sandwich immunoassay.

A) A sandwich MSD immunoassay using rabbit polyclonal anti-GP was developed. To validate specificity, synthetic peptides representing each possible c9RAN protein translated from sense or antisense transcripts of the expanded *C9ORF72* repeat were diluted in Tris-buffered saline (TBS) and assayed (200 ng/ml, 50 µl per well in duplicate wells). Response values correspond to intensity of emitted light upon electrochemical stimulation of the assay plate using the MSD Sector Imager 2400, from which the background response in wells containing only TBS was subtracted. **B)** Poly(GP) protein expression in frontal cortical homogenates from 6 c9FTD/ALS patients and 4 patients without the *C9ORF72* repeat expansion were analyzed by poly(GP) MSD immunoassay. Response values correspond to the intensity of emitted light upon electrochemical stimulation of the assay plate, from which the average background response measured in brain lysates lacking the *C9ORF72* mutation was subtracted. $^{###}$P=0.0002 (non-paired, two-tailed t test). **C)** Standard curve using $(GP)_8$ peptide as the calibrator. A sigmoidal dose-response nonlinear regression was used to fit log(dose) vs. response curve using Prism 5 software. Vertical lines indicate interpolated concentration of poly(GP) in c9ALS CSF (see Table S4).

Table S1. Thermodynamic properties of r(GGGGCC)$_n$ repeats

Oligo nucleotides	Δ*H* (kcal/mol)	Δ*S* (cal/K·mol)	Δ*G* (kcal/mol, 37°C)	T_m (°C, 100 μM)
r(GGGGCC)$_4$[a]	-54.5 ± 1.7	-158 ± 5	-5.69 ± 0.23	73.5 ± 0.6
r(GGGGCC)$_6$[a]	-61.9 ± 2.0	-175 ± 6	-7.54 ± 0.08	79.8 ± 0.3
r(GGGGCC)$_8$[a]	-69.4 ± 0.8	-194 ± 2	-9.26 ± 0.14	81.0 ± 0.5
r(GGGGCC)$_8$[b]	-	-	-	-

[a] RNA samples were heated at 95°C in 10 mM Tris HCl buffer, pH 7.4 and 100 mM NaCl prior to completing optical melting experiments. [b] RNA samples were heated at 95°C in 10 mM Tris HCl buffer, pH 7.4 and 100 mM KCl prior to completing optical melting experiments, the RNA was too stable to observe melting at highest temperature tested (95°C) and thermodynamic parameters were not calculated. All data was recorded in duplicate and presented as mean ± SD.

Table S2. Compounds screened for displacing TO-PRO-1 from r(GGGGCC)$_8$ at different concentrations.

NSC Identifier	Manuscript ID	NSC Identifier	Manuscript ID	NSC Identifier	Manuscript ID
311153	1a	51189	12	211726	23
377363	2	63676	13	215651	24
699145	3	66751	14	220278	25
642	4	66759	15	283167	26
17602	5	66761	16	305831	27
536	6	77880	17	305836	28
35849	7	114702	18	322921	29
38278	8	119095	19	357775	30
41609	9	128584	20	369715	31
50464	10	128801	21	408148	32
50467	11	173329	22		

Table S3. Thermodynamic properties of r(GGGGCC)$_8$ with lead compounds.

Samples[a]	Δ*H* (kcal/mol)	Δ*S* (cal/K·mol)	Δ*G* (kcal/mol, 37°C)	T_m (°C, 100 μM)
r(GGGGCC)$_8$	-71.4 ± 1.4	-201 ± 4	-8.98 ± 0.15	81.6 ± 0.3
r(GGGGCC)$_8$ + **1a**	-74.4 ± 1.0	-208 ± 3	-9.93 ± 0.15	84.7 ± 0.2
r(GGGGCC)$_8$ + **2**	-73.6 ± 0.4	-206 ± 1	-9.61 ± 0.07	83.5 ± 0.1
r(GGGGCC)$_8$ + **3**	-71.1 ± 1.5	-200 ± 4	-9.10 ± 0.24	82.2 ± 0.2

[a] RNA samples (1 μM) were heated at 95°C in 10 mM Tris HCl buffer, pH 7.4 and 100 mM NaCl and cooled to room temperature, followed by addition of the compound (3 μM), then the optical melting experiments were performed. All data was recorded in duplicate and presented as mean ± SD.

Table S4. Patient Information

	C9ORF72 Repeat Expansion	Sample Number	Gender	Age at onset	Age at CSF collection	Estimated [poly(GP)] (ng/ml)
	Yes	1	M	54	56	0.71
	Yes	2	M	49	50	2.49
	Yes	3	F	49	50	97.64
	Yes	4	M	56	56	11.36
	Yes	5	M	58	59	0.12
	Yes	6	M	59	60	0.02
	Yes	7	F	48	48	0.42
	Yes	8	M	42	43	1.03
	Yes	9	F	53	54	1.09
	Yes	10	F	63	64	0.60
	Yes	11	F	60	60	0.13
	Yes	12	F	46	48	3.14
	Yes	13	F	54	57	0.64
	Yes	14	F	53	54	0.63
	No	15	M	54	59	-
	No	16	M	45	47	-
	No	17	F	48	52	-
	No	18	M	57	58	-
	No	19	F	50	52	-
ALS	No	20	M	65	67	-
	No	21	M	59	64	-
	No	22	M	57	59	-
	No	23	M	65	66	-
	No	24	M	74	76	-
	No	25	F	50	51	-
	No	26	F	64	64	-
	No	27	F	65	66	-
	No	28	F	29	29	-
	No	29	M	52	53	-
	No	30	M	36	42	-
	No	31	F	53	57	-
	No	32	M	59	60	-
	No	33	F	55	61	-
	No	34	M	55	55	-
	No	35	M	45	49	-
	No	36	M	65	65	-
	No	37	F	62	63	-
	No	38	M	49	50	-
	No	39	M	76	78	-
healthy	No	40	M	-	68	-
	No	41	M	-	54	-
	No	42	F	-	58	-
	No	43	F	-	51	-
	No	44	M	-	66	-